

Competition between superconductivity and magnetism in
 $\text{RuSr}_2\text{Gd}_{1.5}\text{Ce}_{0.5}\text{Cu}_2\text{O}_{10-\delta}$ (Ru-1222) Rutheno-cuprate compounds

V.P.S. Awana^{*}, M.A. Ansari, Anurag Gupta, R.B. Saxena, and H. Kishan

National Physical Laboratory K.S. Krishnan Marg, New Delhi 110012, India.

and

Devendra Buddhikot and S.K. Malik

Tata Institute of Fundamental Research Homi Bhabha Road, Mumbai 400005,

India.

The $\text{RuSr}_2\text{Gd}_{1.5}\text{Ce}_{0.5}\text{Cu}_2\text{O}_{10-\delta}$ (Ru-1222) compounds with varying oxygen content crystallize in a tetragonal crystal structure (space group *I4/mmm*). Resistance (R) versus temperature (T) measurements show that air-annealed samples exhibit superconductivity with superconducting transition temperature (T_c) onset at around 32 K and $R = 0$ at 3.5 K. On the other hand, N_2 -annealed sample is semiconducting down to 2 K. Magneto-transport measurements on air-annealed sample in applied magnetic fields of 3 and 6 Tesla show a decrease in both T_c onset and $T_{R=0}$. Magneto resistance of up to 20% is observed in N_2 -annealed sample at 2 K and 3 T applied field. The DC magnetization data (M vs. T) reveal magnetic transitions ($T_{\text{mag.}}$) at 100 K and 106 K, respectively, for both air- and N_2 -annealed samples. Ferromagnetic components in the magnetization are observed for both samples at 5K and 20 K. The superconducting transition temperature (T_c) seems to compete with the magnetic transition temperature ($T_{\text{mag.}}$). Our results show that the magnetic ordering temperature ($T_{\text{mag.}}$) of Ru moments in RuO_6 octahedra might have direct influence/connection with the appearance of superconductivity in Cu-O₂ planes of Ru-1222 compounds.

- ❖ Key words: Ruthenocuprates, Superconductivity and Magnetism, Magneto transport and Magneto resistance.
- ❖ PACS: 74.25. *Ha*, 74.72. *Jt*, 75.25. *+z*, 75.30. *Cr*.

Corresponding Author: E-mail: awana@mail.nplindia.ernet.in

1. INTRODUCTION

Recent discovery of the co-existence of magnetism and superconductivity in Ru-1222 ($\text{RuSr}_2(\text{Gd,Ce})_2\text{Cu}_2\text{O}_{10-\text{d}}$) [1,2] and Ru-1212 ($\text{RuSr}_2\text{GdCu}_2\text{O}_{8-\text{d}}$) [3-6] Rutheno-cuprates HTSc compounds has attracted a lot of attention. Both Ru-1212 and Ru-1222 compounds are related with Cu-1212 ($\text{CuBa}_2\text{RECu}_2\text{O}_7$ or RE-123, RE = rare earths) structure with Ba replaced by Sr and oxygen deficient $\text{CuO}_{1-\text{d}}$ chains replaced by RuO_6 octahedra. Further, the oxygen free RE layer between CuO_2 planes is replaced with a rocksalt O-(Gd,Ce)-O block in Ru-1222 structure. Synthesis of both of these compounds in pure phase has been a problem due to formation of magnetic SrRuO_3 and $\text{Gd}_2\text{SrRuO}_6$ in the matrix [1-6].

It is by now widely accepted [1,2, 4-7] that Ru moments in RuO_6 octahedra of Ru-1212/1222 order magnetically around 100-140 K ($T_{\text{mag.}}$), though the exact nature of ordering is still debated [8-10]. Further, superconductivity is observed in the CuO_2 planes with transition temperature (T_c) of up to 40 K [1-10]. Co-existence of superconductivity and magnetism in these compounds has indirectly been proved by nuclear magnetic resonance (NMR) experiments [11]. At the same time, it is worth mentioning that there exist some reports, which are against the genuine co-existence of superconductivity with magnetism in these compounds [12,13].

Both magnetic ordering temperature ($T_{mag.}$) of Ru moments and the superconductivity (T_c) in CuO_2 planes must be controlled by the extent of $\text{Ru}^{4+}/\text{Ru}^{5+}$ ratio in RuO_6 octahedra. The controlling of $T_{mag.}$ is due to mixed $\text{Ru}^{4+}/\text{Ru}^{5+}$ ratio and the T_c due to doping of CuO_2 superconducting planes by charge transfer from RuO_6 octahedra. Oxygen content of RuO_6 octahedra or the ratio of $\text{Ru}^{4+}/\text{Ru}^{5+}$ can be controlled to some extent in Ru-1222, but not in Ru-1212 [14]. Therefore, it is of prime interest to vary the oxygen content of RuO_6 octahedra, and as a result the $T_{mag.}$ and T_c of the Ru-1222 compound. This is the aim of our present article. We successfully controlled the T_c of Ru-1222 from 3.5K to non-superconducting within the same crystallographic phase. This provided us an opportunity to compare the T_c and $T_{mag.}$ of Ru-1222. Our results indicated that both T_c and $T_{mag.}$ compete with each other.

2. EXPERIMENTAL DETAILS

The $\text{RuSr}_2\text{Gd}_{1.5}\text{Ce}_{0.5}\text{Cu}_2\text{O}_{10-\delta}$ (Ru-1222) samples were synthesized through a solid-state reaction route from RuO_2 , SrCO_3 , Gd_2O_3 , CeO_2 and CuO . Calcinations were carried out on the mixed powder at 1000, 1020, 1040 and 1050 $^{\circ}\text{C}$ each for 24 hours with intermediate grindings. The pressed circular pellets were annealed in air for over 48 hours at 1050 $^{\circ}\text{C}$ and are named “air-annealed”. One of the air-annealed pellets was further annealed in nitrogen gas (1 atm) at 420 $^{\circ}\text{C}$ for 24 hours and subsequently cooled slowly to room temperature, named “ N_2 -annealed”. X-ray diffraction (XRD) patterns were obtained at room temperature (MAC Science: MXP18VAHF²²; CuK_{α} radiation). Magnetization measurements were performed on a SQUID magnetometer (Quantum Design: MPMS-5S). Resistivity measurements

under applied magnetic fields of up to 6 T were made in the temperature range of 2 to 300 K using a four-point-probe technique.

3. RESULTS AND DISCUSSION

3a: X-ray diffraction and Phase formation

Both air and N₂-annealed Ru-1222 compounds crystallize in a tetragonal structure (space group I4/mmm) with $a = b = 3.8427(7)$ Å and $c = 28.4126(8)$ Å for the former and $a = b = 3.8498(3)$ Å and $c = 28.4926(9)$ Å for later. An increase in lattice parameters of N₂-annealed sample indicates an overall decrease in oxygen content of the sample. X-ray diffraction patterns for both the air and N₂ -annealed samples are shown in Fig. 1. Small impurities peaks (marked with “*”) are seen close to the background. Presence of small amounts of SrRuO₃ and/or GdSr₂RuO₆ in Ru-1222 samples has been noted earlier also in various reports [1,2,5]. Our currently studied samples are, in fact, far better in terms of their phase purity, compared to those reported earlier by various authors. Ru-1222 is structurally related to the Cu-1212, e.g. CuBa₂YCu₂O_{7-δ} phase with Cu in the charge reservoir replaced by Ru such that the Cu-O chain is replaced by a RuO₂ sheet. Furthermore, a three-layer fluorite-type block, instead of a single oxygen-free *R* (= rare earth element) layer, is inserted between the two CuO₂ planes of the Cu-1212 structure [15] to get Ru-1222 phase.

3b: Electrical transport under magnetic field and Magnetism

The resistance versus temperature (R-T) behavior of air-annealed Ru-1222 sample in magnetic fields of 0, 3 and 6 Tesla in the temperature range of 2-300 K is

shown in Fig.2. The resistance of the compound increases with decrease in temperature indicating its semiconducting behavior. However, in zero applied field, the compound shows a sharp drop in its resistance at around 35 K (T_c onset) and T_c ($R = 0$) at 3.5 K. In applied magnetic fields of 3 and 6 Tesla, though the normal state (above T_c onset) behavior is essentially the same as in zero field, both T_c (onset) and T_c ($R = 0$) decrease with applied field. For example T_c (onset) is 32 K, 27 K and 15 K respectively for 0, 3 and 6 Tesla applied fields and T_c ($R = 0$) state is not observed under these applied magnetic fields. Magneto-resistance, (MR), defined as

$$MR\% = [(R_H - R_0)/R_H] \times 100 \quad (1).$$

is plotted in inset of Fig.2. Though the observed MR% is small, it changes sign at around 180 K. Above 180 K the MR is positive and below 180K it is negative. The change in sign of MR at 180 K might be related to the magnetic structure transformation at the said temperature. This we will be discuss later after magnetization results.

Figure 3 depicts the resistance versus temperature (R-T) behavior for N_2 -annealed Ru1222 sample in magnetic fields of 0, 3 and 6 Tesla. The R-T behavior of this compound is semiconducting down to 2 K. No superconducting transition is observed in the whole temperature range studied (2-300 K). Further, in low temperature region, an appreciable MR is seen for the N_2 -annealed sample. Magneto-resistance (MR), as a function of applied field, at temperatures of 5 and 10 K, for N_2 -annealed sample, is plotted in inset of Fig.3. MR of >20 % is observed at 5 K in an applied field of up to 9 Tesla. At 2 K, around 20% MR is seen even in low applied field of 3 Tesla (plot not shown).

Figure 4 shows the magnetic susceptibility (χ) vs. temperature (T) behaviour in the temperature range of 2 to 300 K for air-annealed Ru-1222 sample in an applied field of 100 Oe, measured in both zero-field-cooled (ZFC) and field-cooled (FC) modes. The χ vs. T plot shows the branching of ZFC and FC curves at around 95 K. Though the ZFC and FC magnetic susceptibility branching is seen at around 95 K, the magnetic susceptibility starts shooting up at higher temperature of around 100 K (T_{mag}). In fact, the susceptibility of Ru-1222 compound does deviate from normal Curie-Weiss paramagnetic behaviour at around 165 to 200 K. It has been reported that the Ru moments in Ru-1222 order antiferromagnetically at around 180 K, which later develop in to a canted ferromagnetism at lower temperatures (T_{mag}) [1,2,6]. As mentioned earlier, the exact nature of magnetic ordering in low temperature region is still debated. The 180 K paramagnetic to antiferromagnetic transition could be seen in magneto-transport measurements also, where small positive MR changes to negative MR below this temperature (inset, Fig.2).

The characteristic temperature T_{mag} is weakly dependent on applied magnetic field $H < 100$ Oe. For $H > 1000$ Oe, both ZFC and FC magnetization curves are merged with each other (see inset, Fig. 4). In fact, no ZFC - FC branching is observed down to 2 K in 5000 Oe field. This is in general agreement with earlier reports [1,2]. Superconductivity is not seen in terms of diamagnetic transition (T_d) in applied field of $H = 100$ Oe (Fig.4). It is known that, due to internal magnetic field, these compounds are in a spontaneous vortex phase (SVP) even in zero external field [16]. For $T_d < T < T_c$, the compound remains in a mixed state. Hence though $R = 0$ is achieved at relatively higher temperatures (3.5 K, see Fig.2) the diamagnetic response is seen at much lower temperatures and that too in quite small applied magnetic ($H_{c1} < 25$ Oe) fields. Hence we could conclude that the magnetic susceptibility (χ) vs. T

behaviour shown in Fig. 4 does not exclude the presence of superconductivity in air-annealed presently studied Ru-1222 compound. At lower applied field of 5 Oe, the compound exhibits diamagnetic transition (T_d) below $T_c(R=0)$ state (curve not shown).

The χ -T behaviour in the temperature range of 2 to 300 K for N_2 -annealed Ru-1222 sample in an applied fields of 100 Oe, measured in both zero-field-cooled (ZFC) and field-cooled (FC) modes, is shown in Fig.5. The general shape of FC and ZFC magnetization plots is similar to that for Air-annealed sample. The only interesting change is that T_{mag} (defined earlier) has increased to 106 K for N_2 -annealed sample. Worth mentioning is the fact that N_2 -annealed sample is not superconducting down to 2 K (Fig.3, R vs. T results).

3c: Ferromagnetic component

Magnetization (M) versus applied field (H) isotherm at 5 K for air-annealed Ru-1222 sample is shown in Fig. 6. The magnetization starts saturating above 6 Tesla in both directions. The M-H plot is further zoomed in applied field of -900 Oe to 900 Oe, and shown in inset of Fig.6. At 5 K, the returning moment (M_{rem}) i.e. the value of magnetization at zero returning field and the coercive field (H_c) i.e. the value of applied returning field to get zero magnetization are respectively 2.50 emu/gram and 160 Oe (inset Fig.6). It is known that the Gd (magnetic rare earth) in the compound orders magnetically below 2 K and Ce remains in a tetravalent, non-magnetic state, hence the M_{rem} and H_c arising from the ferromagnetic hysteresis loops do belong to Ru only. Interestingly, for Ru-1212, the hysteresis loops are reported to be quite narrow [4,5]. This indicates that in Ru-1222 the ferromagnetic domains are less anisotropic and more rigid. The M-H loop at 20 K for air-annealed sample is shown in Fig. 7, which shows a decreased M_{rem} (1emu/gram) and H_c (75 Oe) compared to 5 K plot in

Fig. 6. The values of both M_{rem} and H_c decrease with T . Hysteresis loops were not seen at higher temperatures above T_{mag} . For example, the M-H plot at 150 K is seen as completely linear with field (Fig. 8), and no hysteresis loops were visible even after zooming at low fields (inset of Fig. 8).

Figure 9 depicts the M-H plot at 5 K for N_2 -annealed sample. This plot is similar to that observed for air-annealed sample. The zoomed ferromagnetic component is shown in the inset. The interesting difference, when compared with air-annealed sample, is that M does not saturate in applied fields up to 7 Tesla. This is in contrast to the M-H plot for air-annealed sample at 5 K for which M saturates in a field of 6 Tesla (see Fig. 6). The M-H plot for N_2 -annealed sample is further zoomed in applied field of -900 Oe to 900 Oe, and shown in the inset of Fig.9. Ferromagnetic loop is seen clearly with M_{rem} (2emu/gram) and H_c (170Oe). The M-H loop at 20 K for N_2 -annealed sample is shown in Fig.10, which reveals decreased M_{rem} (1emu/gram) and H_c (70 Oe). The trend of M_{rem} and H_c for N_2 -annealed sample is similar to that of Air-annealed, i.e both of them decrease with increase in temperature. The M-H loops were not seen above T_{mag} for the N_2 -annealed samples also.

The results shown above for both air- and N_2 -annealed presently studied Ru-1222 samples may be summarised as follows:

1. Both air- and N_2 -annealed samples crystallize in a single phase tetragonal structure (space group I4/mmm).
2. The air-annealed sample is superconducting with $T_c(R=0)$ of 3.5 K, while the N_2 -annealed is not superconducting down to 2 K. N_2 -annealed sample exhibits negative magneto-resistance of up to 20% at 5 K.

3. Both air- and N₂-annealed samples order magnetically, with T_{mag} of nearly 100 K for the former and 106 K for the later.
4. Both air- and N₂-annealed samples exhibit ferromagnetic loops below T_{mag}. The relative width of loops is more (higher M_{rem} and H_c) for air-annealed sample compared to that of N₂-annealed sample at a fixed temperature.
5. For air-annealed sample, the M-H behaviour at 5 K exhibits near saturation above 6 Tesla. However, for N₂-annealed sample, M is not saturated up to applied field of 7 Tesla.

We now discuss these points one by one. As far as phase formation and the crystallization of the two Ru-1222 samples is concerned, it seems there is some scope for oxygen to get released from RuO₆ octahedra while still maintaining its crystal structure. In fact, another thought of school also exists, which believes in release of oxygen from rocksalt O-(Gd,Ce)-O block and not from RuO₆ in Ru-1222. Recent spectroscopic studies on Ru-1222 do show indications towards valence fluctuations of Ru⁴⁺/Ru⁵⁺ and hence some variation in oxygen of RuO₆ octahedra [17]. It has been reported earlier that oxygen content of Ru-1222 is tunable to some extent by N₂/Ar₂ annealing but not for Ru-1212.[14]. Thus it has been possible for us, in the present study, to get both air- and N₂-annealed Ru-1222 samples in the same crystal structure. Decreased oxygen content of N₂-sample is indicated by increased c-parameter of the sample (the exact oxygen content has not been determined).

As far as the second point is concerned, the air-annealed sample is superconducting but N₂-annealed sample is not. Further, the normal state conduction, though semiconducting for both samples, is relatively better for air-annealed sample. This indicates that air-annealed sample has relatively more mobile hole-carriers than

the N_2 -annealed sample. The doping of mobile holes in widely believed conducting/superconducting $Cu-O_2$ planes in RE-123 compounds takes place by charge transfer from oxygen variable redox CuO_{1-d} chains. In Ru-1222, the role of redox layer is supposedly played by RuO_6 octahedra. In N_2 -annealed sample the Ru^{4+}/Ru^{5+} ratio will be different than in air-annealed sample, and hence there will be different number of transferred mobile holes to $Cu-O_2$ planes. As far as magneto-transport is concerned, no appreciable MR is seen above T_{mag} for both the samples. For air-annealed superconducting sample, the broadening of transition under field is seen and is similar to that in other HTSC compounds. For N_2 -annealed sample, negative MR of around 20% is seen at 2 K. As we know from present magnetization measurements and various other reports earlier, that the low temperature magnetism of Ru-1222 is complex and calls for magnetic phase separation including spin glass [10], canted antiferromagnetism [18], or both simultaneously. Though magnetic structure of Ru-1222 is not yet revealed by low temperature neutron scattering measurements, one thing is apparent that the compound possesses complex low temperature magnetism. In such situations appreciable MR is expected due to tunnelling between various magnetic domains arising from magnetically phase separated system. The N_2 -annealed sample is highly under-doped and hence one presumes that electrical transport conduction is mainly through RuO_6 layer, where magnetic scattering does take place. The role of magnetic charge spin scattering has earlier been observed in Ru-1212, where T_{mag} is seen clearly as a hump in resistivity measurements [4,12]. To our knowledge this is the first observation of finding appreciable negative MR at 2K in a non-superconducting Ru-1222 compound. This is in conformity with the earlier reports of magnetic phase separation at low temperature in Ru-1222 [17,18].

Third point comprises of the fact that, for superconducting air-annealed sample, T_{mag} is 100 K while the same is 106 K for non-superconducting N_2 -annealed sample. As discussed in point 1 above, the $\text{Ru}^{4+}/\text{Ru}^{5+}$ ratio in both the samples is supposed to be different. The amount of Ru^{4+} will be higher in N_2 -annealed sample [14,17]. T_{mag} originates from the ordering of Ru moments in RuO_6 octahedra. Changed amount of $\text{Ru}^{4+}/\text{Ru}^{5+}$ magnetic spins contribution is responsible for different T_{mag} of the two compounds. Higher content of Ru^{4+} gives rise to increased T_{mag} .

Fourth point says that though both compounds have ferromagnetic domains at low temperatures below T_{mag} , the characteresitc values of M_{rem} and H_c are relatively higher for air-annealed sample. Our detailed micro-structural studies earlier for Ru-1222 showed that the observed super-lattice structures due to tilt of RuO_6 octahedra [19] might be coupled with the weak ferromagnetic domains constructed by ordering of the canted Ru moments below the magnetic transition temperature (T_{mag}). Hence ferromagnetic domains coupling depends on the long range ordering of tilted RuO_6 octaherdas in a given Ru-1222 system. In N_2 -annealed sample, the long-range superstructures may break down relatively at smaller length scale than for air-annealed sample due to less oxygen in RuO_6 octahedra of the same giving rise to weak coupling of the ferromagnetic domains. This will give rise to lower values of M_{rem} and H_c . This also explains the fifth point regarding the observed saturation of M-H curve for air-annealed sample and not for N_2 -annealed sample. The saturation of M-H is dependent on the long range coupling of aligned ferromagnetic domains, which is observed for air-annealed sample only. Long range coupling of aligned moments is directly dependent on the stability of RuO_6 octahedra tilt angle superstructures, which is certainly less for N_2 - annealed sample due to break down in homogenous oxygen content close to 6.0 in the octahedra.

6. FIGURE CAPTIONS

Figure 1. X-ray diffraction pattern observed for the air- and N_2 – annealed Ru-1222 samples.

Figure 2. Resistance (R) vs. temperature (T) plots in 0, 3, and 6 T applied magnetic fields for air-annealed Ru-1222. Inset shows the Magnetoresistance (MR%) vs. T plot for 6 Tesla applied field.

Figure 3. Resistance (R) vs. temperature (T) plots in 0, 3, and 6 T applied magnetic fields for N_2 -annealed Ru-1222. Inset shows the Magnetoresistance (MR%) at 5 K in applied fields up to 9 Tesla.

Figure 4. Magnetic susceptibility (χ) vs. temperature (T) plot for air-annealed Ru-1222 in both ZFC and FC modes with applied field of 100 Oe, inset shows the same for $H = 5000$ Oe.

Figure 5. Magnetic susceptibility (χ) vs. temperature (T) plot for N_2 – annealed Ru-1222 in both ZFC and FC modes with applied field of 100 Oe.

Figure 6. Magnetization-Field (M–H) hysteresis loop for air-annealed Ru-1222 sample at 5 K. Inset shows the same for -900 Oe = $H = +900$ Oe.

Figure 7. Magnetization-Field (M–H) hysteresis loop for air-annealed Ru-1222 sample at 20 K Inset shows the same for -900 Oe = $H = +900$ Oe.

Figure 8. Magnetization-Field (M–H) hysteresis loop for air-annealed Ru-1222 sample at 150 Inset shows the same for -900 Oe = $H = +900$ Oe.

Figure 9. Magnetization-Field (M–H) hysteresis loop for N_2 -annealed Ru-1222 sample at 5 K Inset shows the same for -900 Oe = $H = +900$ Oe.

Figure 10. Magnetization-Field (M–H) hysteresis loop for N_2 -annealed Ru-1222 sample at 20 K. Inset shows the same for -900 Oe = $H = +900$ Oe.

REFERENCES

1. I. Felner, U. Asaf, Y. Levi, and O. Millo, Phys. Rev. B 55, R3374 (1997)
2. I. Felner, and U. Asaf, Int. J. Mod. Phys. B. 12, 3220 (1998)
3. L. Bauernfeind, W. Widder and H.F. Braun, Physica C 254, 151 (1995).
4. C. Bernhard, J.L. Tallon, Ch. Niedermayer, Th. Blasius, A. Golnik, E. Brücher, R.K. Kremer, D.R. Noakes, C.E. Stronack, and E.J. Asnaldo, Phys. Rev. B 59, 14099 (1999).
5. J. L. Tallon, J. W. Loram, G.V.M. Williams, and C. Bernhard, Phys. Rev. B 61, R6471 (2000)
6. V.P.S. Awana, S. Ichihara, J. Nakamura, M. Karppinen, and H. Yamauchi, Physica C 378-381, 249-254 (2002).
7. A. Butera, A. Fainstein, E. Winkler, and J. Tallon, Phys. Rev. B 63, 54442 (2001)
8. J.W. Lynn, B. Keimer, C. Ulrich, C. Bernhard, and J.L. Tallon, Phys. Rev. B 61, R14964 (2000).
9. V.P.S. Awana, T. Kawashima and E. Takayama-Muromachi, Phys. Rev. B. 67, 172502 (2003).
10. C. A. Cardoso, F.M. Araujo-Moreira, V.P.S. Awana, E. Takayama-Muromachi, O.F. de Lima, H. Yamauchi, M. Karppinen, Phys. Rev. B 67, 024407R (2003).
11. Y. Tokunaga, H. Kotegawa, K. Ishida, Y. Kitaoka, H. Takigawa, and J. Akimitsu, Phys. Rev. Lett. 86, 5767 (2001).
12. V.P.S. Awana, S. Ichihara, J. Nakamura, M. Karppinen, H. Yamauchi, Jinbo Yang, W.B. Yelon, W.J. James and S.K. Malik, J. Appl. Phys. 91, 8501 (2002).

13. C.W. Chu, Y.Y. Xue, S. Tsui, J. Cmaidalka, A.K. Heilman, B. Lorenz, and R.L. Meng, *Physica C* 335, 231 (2000).
14. M. Matvejeff, V.P.S. Awana, H. Yamauchi and M. Karppinen, *Physica C* 392-396, 87-92 (2003).
15. N. Sakai, T. Maeda, H. Yamauchi and S. Tanaka, *Physica C* 212, 75 (1993).
16. E.B. Sonin, and I. Felner, *Phys. Rev. B* 57, R14000 (1998).
17. V.P.S. Awana, M. Karppinen, H. Yamauchi, R.S. Liu, J.M. Chen and L.-Y. Jang, *J. Low Temp. Physics* 131, 1211 (2003).
18. I. Živkovic, Y. Hirai, B.H. Frazer, M. Prester, D. Drobac, D. Ariosa, H. Berger, D. Pavuna, G. Margaritondo, I. Felner and M. Onellion, *Phys. Rev. B* 65, 144420 (2002).
19. Tadahiro Yokosawa, Veer Pal Singh Awana, Koji Kimoto, Eiji Takayama-Muromachi, Maarit Karppinen, Hisao Yamauchi and Yoshio Matsui, Accepted in *Ultramicroscopy* (2003).

Fig.1 Awana et al.

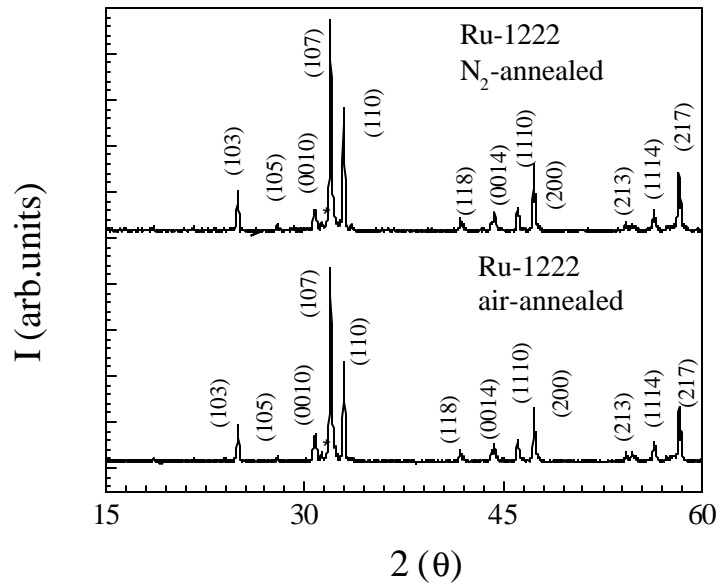


Fig.2 Awana et al.

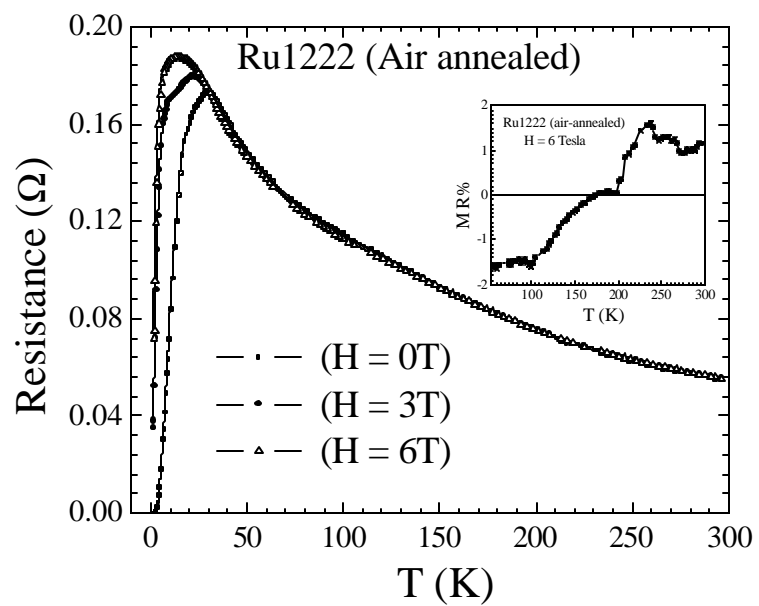


Fig.3 Awana et al.

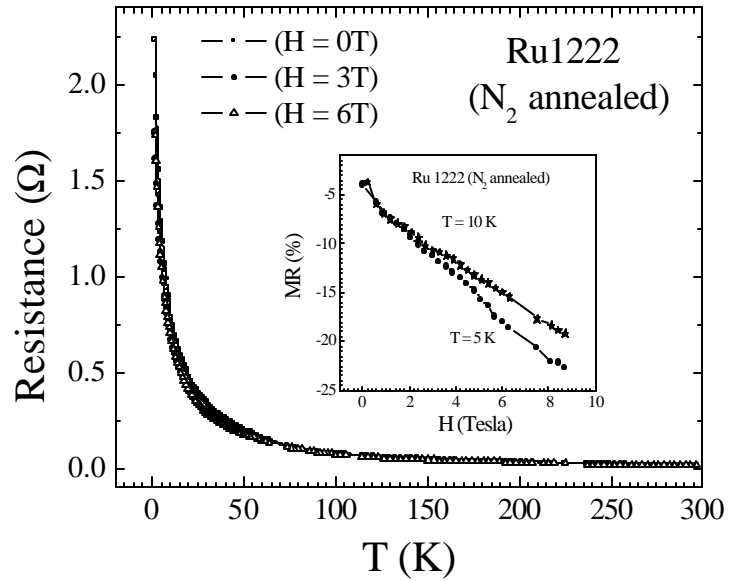


Fig.4 Awana et al.

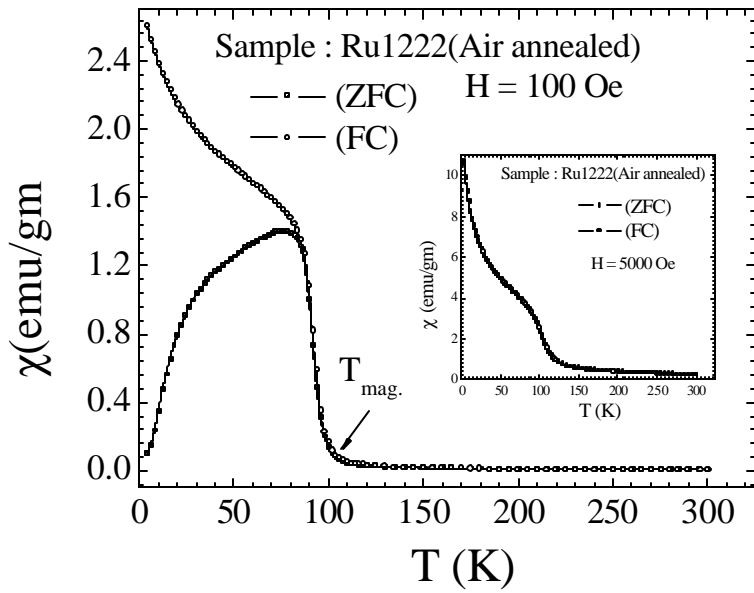


Fig.5 Awana et al.

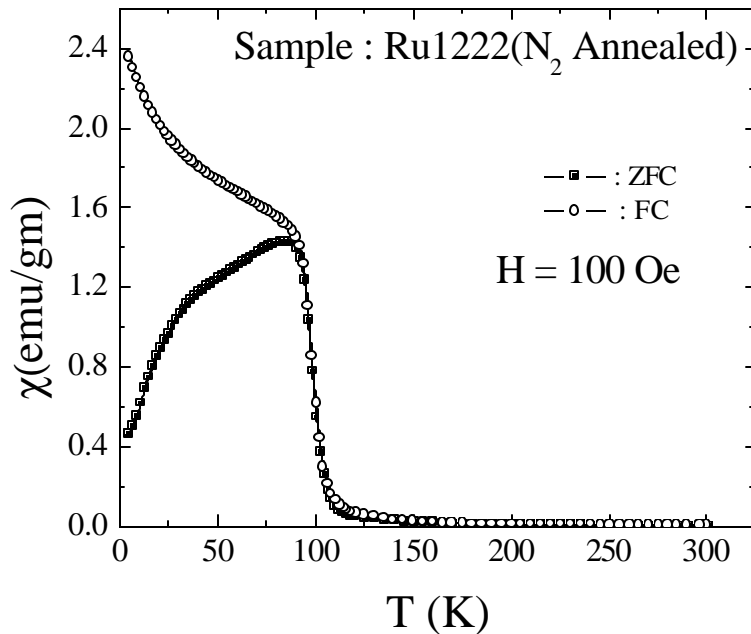


Fig.6 Awana et al.

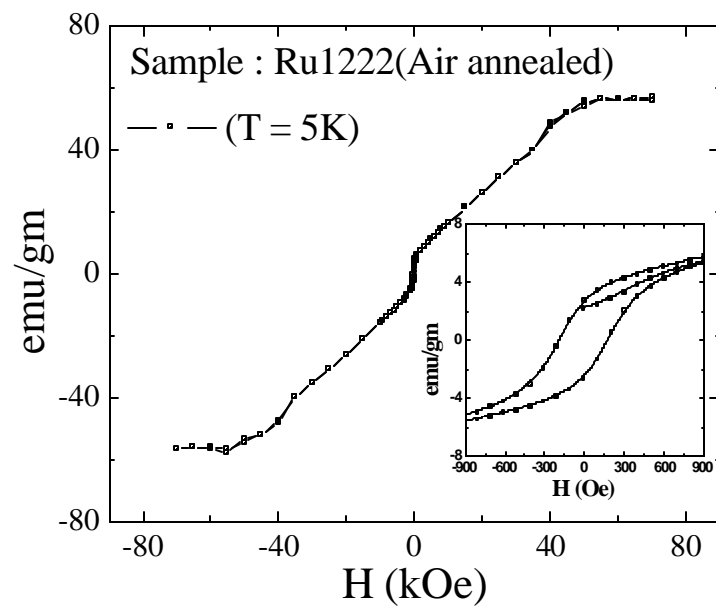


Fig.7 Awana et.al.

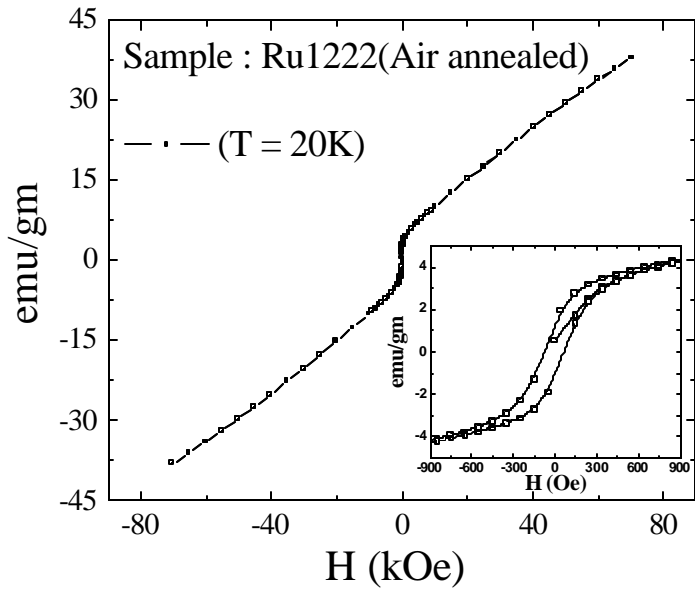


Fig.8 Awana et.al.

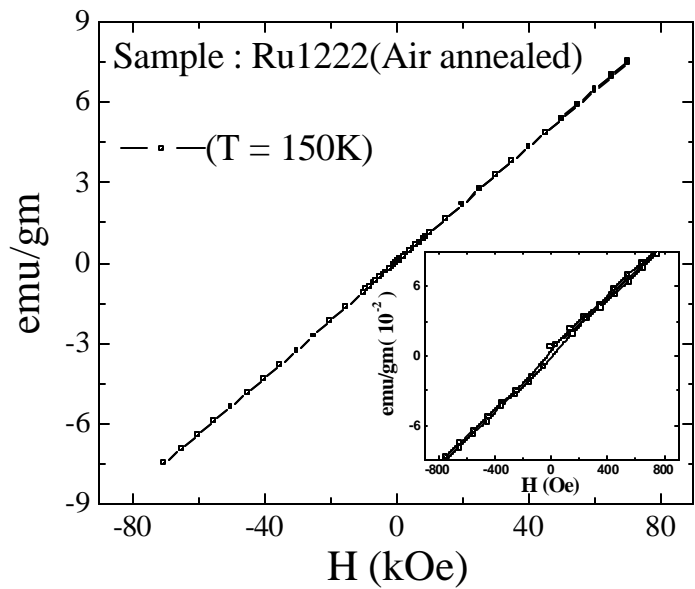


Fig.9 Awana et.al.

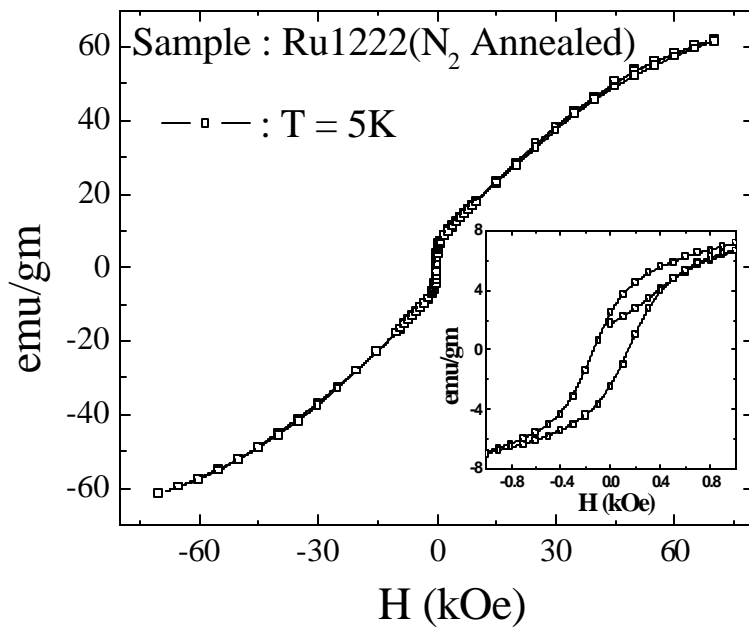


Fig.10 Awana et.al.

